Available online at www.sciencedirect.com

SciVerse ScienceDirect

Solar Energy 86 (2012) 2695–2706

SOLAR ENERGY

www.elsevier.com/locate/solener

A cell-to-module-to-array detailed model for photovoltaic panels

Hongmei Tian [a,b], Fernando Mancilla-David [a,*], Kevin Ellis [d], Eduard Muljadi [c], Peter Jenkins [d]

[a] Department of Electrical Engineering, University of Colorado Denver, 1200 Larimer St., Denver, CO 80217, USA
[b] Industrial Training Center, Shenzhen Polytechnic, Xili Lake, Shenzhen, Guangdong 518055, China
[c] National Renewable Energy Laboratory, 1617 Cole BLVD, Golden, CO 80401, USA
[d] Mechanical Engineering Department, University of Colorado Denver, 1200 Larimer St., Denver, CO 80217, USA

Received 17 April 2012; received in revised form 6 June 2012; accepted 7 June 2012
Available online 30 June 2012

Communicated by: Associate Editor Nicola Romeo

Abstract

This paper presents a modified current–voltage relationship for the single-diode model. The single-diode model has been derived from the well-known equivalent circuit for a single photovoltaic (PV) cell. A cell is defined as the semiconductor device that converts sunlight into electricity. A PV module refers to a number of cells connected in series and in a PV array, modules are connected in series and in parallel. The modification presented in this paper accounts for both parallel and series connections in an array. Derivation of the modified current–voltage relationships begins with a single solar cell and is expanded to a PV module and finally an array. Development of the modified current–voltage relationship was based on a five-parameter model, which requires data typically available from the manufacturer. The model accurately predicts voltage–current (V–I) curves, power–voltage (P–V) curves, maximum power point values, short-circuit current and open-circuit voltage across a range of irradiation levels and cell temperatures. The versatility of the model lies in its accurate prediction of the aforementioned criteria for panels of different types, including monocrystalline and polycrystalline silicon. The model is flexible in the sense that it can be applied to PV arrays of any size, as well as in simulation programs such as EMTDC/PSCAD and MatLab/Simulink. Accuracy of the model was validated through a series of experiments performed outdoors for different configurations of a PV array.

Keywords: Solar cell; Photovoltaic module; Photovoltaic array; PV system simulation; Mathematical PV model; Outdoor measurement

1. Introduction

Growing interest in renewable energy resources has caused the photovoltaic (PV) power market to expand rapidly, especially in the area of distributed generation. For this reason, designers need a flexible and reliable tool to accurately predict the electrical power produced from PV arrays of various sizes. A *cell* is defined as the semiconductor device that converts sunlight into electricity. A PV module refers to a number of cells connected in series and in a PV array, modules are connected in series and in parallel. Most of the mathematical models developed are based on current–voltage relationships that result from simplifications to the double-diode model proposed by Chan and Phang (1987). The current–voltage relationship for the single-diode model assumes that one lumped diode mechanism is enough to describe the characteristics of the PV cell. This current–voltage relationship is the basis for

* Corresponding author. Tel.: +1 303 556 6674; fax: +1 303 556 2383.
E-mail addresses: hmtian@szpt.edu.cn (H. Tian), Fernando.Mancilla-David@ucdenver.edu (F. Mancilla-David), kevin.ellis86@gmail.com (K. Ellis), eduard.muljadi@nrel.gov (E. Muljadi), Peter.Jenkins@ucdenver.edu (P. Jenkins).

0038-092X/$ - see front matter © 2012 Elsevier Ltd. All rights reserved.
http://dx.doi.org/10.1016/j.solener.2012.06.004

Nomenclature

α_T	temperature coefficient of short-circuit current
α'_T	relative temperature coefficient of short-circuit current
β'_T	relative temperature coefficient of open-circuit voltage
β_T	temperature coefficient of open-circuit voltage
γ_C	cell efficiency
ref	variable at SRC
E_g	bandgap energy (eV)
G_T, G	solar irradiance/irradiation $\left(\frac{W}{m^2}\right)$
I_{dio}	current through anti-parallel diode
I_{irr}	photocurrent
I_{MP}	maximum power point current
I_O	diode saturation current
I_p	shunt current due to shunt resistor branch
I_{SC}	short-circuit current
k	Boltzmann's constant ($k = 1.3806503 \times 10^{-23}$ J/K)
n	ideality factor
N_C	number of cells in series in each module
N_M	number of modules in series
N_P	number of strings in parallel
N_S	number of cells in series
$NOCT$	Nominal Operating Condition $\left(G_{NOCT} = 800\frac{W}{m^2}, T_{a,NOCT} = 20\,^{\circ}\text{C}, AM = 1.5\right)$
q	electronic charge ($q = 1.602 \times 10^{-19}$ C)
R_P	shunt resistance
R_S	series resistance
T	cell temperature (°C)
$T_{a,NOCT}$	ambient temperature at $NOCT$ conditions ($Ta,NOCT = 20\,^{\circ}\text{C}$)
T_a, T_{amb}	ambient temperature (°C)
T_{NOCT}, $NOCT$	nominal operating cell temperature (°C)
$U_{L,NOCT}$	loss coefficient at $NOCT$ conditions
U_L	loss coefficient at operating conditions
V_{MP}	maximum power point voltage
V_{OC}	open-circuit voltage
$(\tau\alpha)$	absorptance–emittance product
array	any number of modules connected in series and in parallel
cell	semiconductor device that converts sunlight into electricity module any number of solar cells in series
SRC	Standard Reference Condition $\left(G_{ref} = 1000\frac{W}{m^2}, T_{ref} = 25\,^{\circ}\text{C}\right)$

the mathematical models developed by Desoto et al. (2006) and Jain and Kapoor (2004). Further simplification to the current–voltage relationship is made by assuming the shunt resistance is infinite, thus forming the basis for the four parameter mathematical model. Numerous methods have been developed to solve this particular model. Khezzar et al. (2009) developed three methods for solving the model. Chenni et al. (2007) developed a simplified explicit method by assuming that the photocurrent (I_{irr}) is equal to the short-circuit current (I_{SC}). Zhou et al. (2007) introduced the concept of a Fill Factor (FF) to solve for the maximum power-output (P_{Max}).

Rajapakse and Muthumuni (2009) developed a model based on the current–voltage relationship for the single diode in EMTDC/PSCAD. Campbell (2007) developed a circuit-based, piecewise linear PV device model, which is suitable for use with converters in transient and dynamic electronic simulation software. King (1997) developed a model to reproduce the V–I curve using three important points: short-circuit, open-circuit, and maximum power point conditions on the curve. To improve accuracy, King et al. (2004) expanded the model to include two additional points along the V–I curve. However, the method requires, in addition to the standard parameters such as the series resistance (R_S) and shunt resistance (R_P), empirically determined coefficients that are provided by the Sandia National Laboratory. The model proposed by King et al. (2004) is ideal for cases where the PV array will be operating at conditions other than the maximum power point.

The US Department of Energy (DOE) supported recent development of the Solar Advisor Model (SAM). SAM provides three options for module performance models: the Sandia Performance Model proposed by King et al. (2004), the five parameter model popularized by Desoto et al. (2006) and a single-point efficiency model. The single-point efficiency model is used for analysis where the parameters required by other models are not available. Cameron et al. (2008) completed a study comparing the three performance models available in SAM with two-other DOE-sponsored models: PVWATTS is a simulation program developed by the National Renewable Energy Laboratory and PVMOD is a simulation program developed by the Sandia National Laboratory. Both programs can be found on the respective laboratory website. The study compared the predicted results with actual measured results from a PV array; all were found to agree with minimal deviation from the measured values. For this study, the modified current–voltage relationship was solved using a method based on the five parameter model since it only requires data provided by the manufacturer and has been shown to agree well with measured results.

In this study, a modified current–voltage relationship for a single solar cell is expanded to a PV module and finally to a PV array. The five parameter model given by Desoto

et al. (2006) uses the current–voltage relationship for a single solar cell and only includes cells or modules in series. This paper presents a modification to this method to account for both series and parallel connections. Detailed current–voltage output functions are developed for a cell, a module and a string of modules connected in series and in parallel. This cell-to-module-to-array model makes the similarities and differences of the equivalent circuits and current–voltage relationships clear.

Manufacturers typically provide the following operational data on PV panels: the open-circuit voltage (V_{OC}); the short-circuit current (I_{SC}); the maximum power point current (I_{MP}) and voltage (V_{MP}); and the temperature coefficients of open-circuit voltage and short-circuit current (β_T and α_T, respectively). This operational data is required to solve the improved five parameter determination method. The model predicted V–I curves, P–V curves, maximum power point, short-circuit current, and open-circuit voltage conditions across a range of irradiation levels and cell temperatures are used for comparison with the experimental data provided by the manufacturer. The proposed model can be applied for PV arrays of any size and is suitable for application in simulation programs such as EMTDC/PSCAD and MatLab/Simulink. A series of experiments were performed outdoors for different configurations of a PV array to validate the accuracy of the model. The experiments revealed consistency between experimental and model predicted results for V–I and P–V curves for each configuration.

Overall, this paper makes the following contributions:

- A current source-based PV array model suitable for computer simulations.
- Development of a current–voltage relationship for a PV array.
- Development of a datasheet based parameter determination method.
- Demonstration of the model and validation through experimental results.

2. Development of the modified current–voltage relationship

Designers need a flexible and reliable tool to accurately predict the electrical power produced from a PV array, whether connected in series or parallel.

2.1. Current–voltage relationship for a single solar cell

A solar cell is traditionally represented by an equivalent circuit composed of a current source, an anti-parallel diode, a series resistance and a shunt resistance (Masters, 2004). As shown in Fig. 1, the anti-parallel diode branch is modified to an external control current source which is anti-paralleled with the original current source.

According to Kirchoff's current law,

$$I = I_{irr} - I_{dio} - I_p \tag{1}$$

where I_{irr} is the photo current or irradiance current, which is generated when the cell is exposed to sunlight. I_{irr} varies linearly with solar irradiance for a certain cell temperature. I_{dio} is the current flowing through the anti-parallel diode, which induces the non-linear characteristics of the solar cell. I_p is shunt current due to the shunt resistor R_P branch. Substituting relevant expressions for I_{dio} and I_p, we get

$$I = I_{irr} - I_0\left[\exp\left(\frac{q(V+IR_S)}{nkT}\right) - 1\right] - \frac{V+IR_S}{R_P} \tag{2}$$

where q is the electronic charge ($q = 1.602 \times 10^{-19}$ C), k is the Boltzmann constant ($k = 1.3806503 \times 10^{-23}$ J/K), n is the ideality factor or the ideal constant of the diode, T is the temperature of the cell, I_0 is the diode saturation current or cell reverse saturation current and R_S and R_P represent the series and shunt resistance, respectively.

2.2. Current–voltage relationship for a photovoltaic module

A PV module is typically composed of a number of solar cells in series. N_S represents the number of solar cells in series for one module. For example, $N_S = 36$ for BP Solar's BP365 Module, $N_S = 72$ for ET-Solar's ET Black Module ET-M572190BB, etc. When N_S solar cells are connected in series to build up a module, the output current I_M and output voltage V_M of the module have the following relationship.

$$I_M = I_{irr} - I_0\left[\exp\left(\frac{q(V_M + I_M N_S R_S)}{N_S nkT}\right) - 1\right] - \frac{V_M + I_M N_S R_S}{N_S R_P} \tag{3}$$

This equation can be expanded to any number of cells in series (N_S), and thus is not restricted to one module. If there are N_M modules connected in series, and there are N_C cells in series in each module, then

$$N_S = N_M \times N_C \tag{4}$$

2.3. Current–voltage relationship for a photovoltaic array

In an array, PV modules are connected in series and in parallel. It is important to consider the effects of those connections on the performance of the array. We began with the current–voltage relationship for a single solar cell, connected the cells in series to form a string, and now develop the current–voltage relationship for groups of strings connected in parallel (an array). With reference to Fig. 2, the output current I_A and output voltage V_A of a PV array with N_S cells in series and N_P strings in parallel is found from the following equation

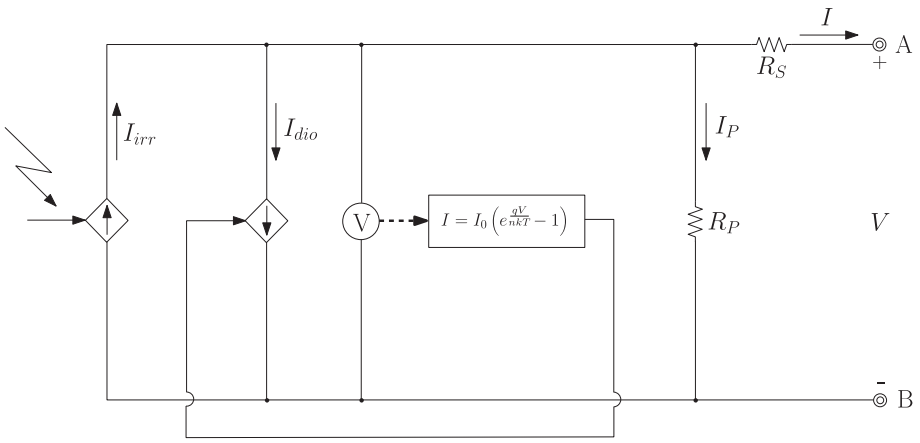

Fig. 1. Modified equivalent circuit for a solar cell.

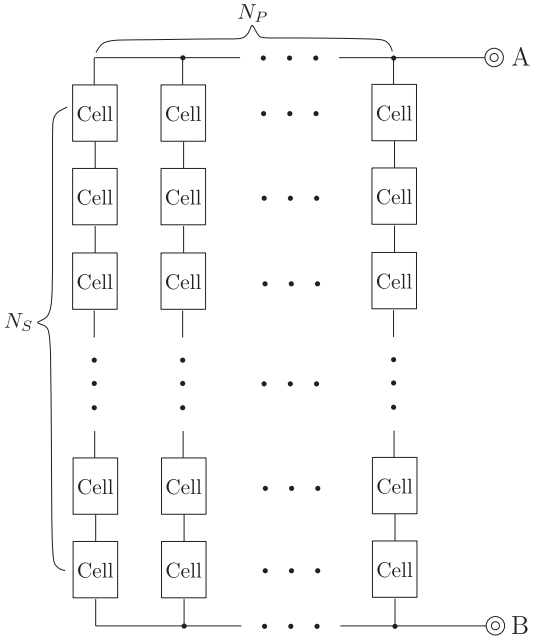

Fig. 2. Physical configuration of a PV array.

$$I_A = N_P I_{irr} - N_P I_0 \left[\exp\left(\frac{q(V_A + I_A \frac{N_S}{N_P} R_S)}{N_S nkT}\right) - 1\right] - \frac{V_A + I_A \frac{N_S}{N_P} R_S}{\frac{N_S}{N_P} R_P} \quad (5)$$

Comparing (5) with (2), it is clear the equations have similar forms. In electromagnetic transient simulation programs such as EMTDC/PSCAD and MatLab/Simulink, the model of a PV array can be built directly using (5). After adopting the substitutions in Table 1, (5) can be rewritten as

$$I_A = I'_{irr} - I'_0 \left[\exp\left(\frac{q(V_A + I_A R'_S)}{N_S nkT}\right) - 1\right] - \frac{V_A + I_A R'_S}{R'_P} \quad (6)$$

Following the substitutions outlined in Table 1, the current–voltage relationship given in (6) appears similar to the current–voltage relationship for a single solar cell, and thus the equivalent circuit for the PV array will be similar to the equivalent circuit for a single solar cell (Fig. 1). However, each variable in the circuit shown in Fig. 1 will now have a different meaning based on the substitutions provided in Table 1 and the second external control current source will have a different control scheme.

Table 1
Substitutions for the model of a PV array.

Original expression	Substitution
$N_P I_{irr}$	I'_{irr}
$N_P I_0$	I'_0
$\frac{N_S}{N_P} R_S$	R'_S
$\frac{N_S}{N_P} R_P$	R'_P

3. Important model parameters

Prior to derivation of the cell-to-module-to-array model, it is necessary to discuss the important model parameters and how they change with operating conditions.

3.1. Ideality factor (n)

The ideality factor (n) accounts for the different mechanisms responsible for moving carriers across the junction. The parameter n is 1 if the transport process is purely diffusion and $n \approx 2$ if it is primarily recombination in the depletion region. Some research papers (e.g. Rajapakse and Muthumuni, 2009) suggest an n of 1.3 for silicon. The parameter n represents one of the unknowns of the cell-to-module-to-array model. In our work, n is assumed to be related only to the material of the solar cell and be independent of temperature and solar irradiation.

If values for the photocurrent (I_{irr}), diode saturation current (I_0), series resistance (R_S), and shunt resistance (R_P) are known, along with the operational data provided by the manufacturer (V_{OC}, I_{SC}, I_{MP}, V_{MP}, β_T, α_T), n can be solved for. For example, Jain and Kapoor (2005) used Lambert W-Functions to solve for the ideality factor.

Bashahu and Nkundabakura (2007) assessed the accuracy of 22 different methods for determining the ideality factor for different current–voltage relationships and described the parameter n as a unitless factor defining the extent to which the solar cell behaves as an ideal diode. No matter the operating condition, the value of n will not change. The value of n compared to the value of n_{ref} at Standard Reference Conditions (SRC) is given by,

$$n = n_{ref} \tag{7}$$

where the solar irradiation is $G_{ref} = 1000\ \mathrm{W/m^2}$ and the cell temperature is $T_{ref} = 298\ \mathrm{K}$ or $T_{ref} = 25\ ^\circ\mathrm{C}$ at SRC.

3.2. Photo current I_{irr}

The photo current (I_{irr}) depends on the solar irradiance G and cell temperature T and is given by

$$I_{irr} = I_{irr,ref}\left(\frac{G}{G_{ref}}\right)\left[1 + \alpha'_T(T - T_{ref})\right] \tag{8}$$

where $I_{irr,ref}$ is the photo current at SRC. α'_T is the relative temperature coefficient of the short-circuit current, which represents the rate of change of the short-circuit current with respect to temperature. Manufacturers occasionally provide the absolute temperature coefficient of the short-circuit current, α_T, for a particular panel. The relationship between α'_T and α_T is

$$\alpha_T = \alpha'_T I_{irr,ref} \tag{9}$$

$I_{irr,ref}$ is the second unknown parameter in the model.

3.3. Diode saturation current I_0

I_0 is primarily dependent on the temperature of the cell:

$$I_0 = I_{0,ref}\left[\frac{T}{T_{ref}}\right]^3 \exp\left[\frac{E_{g,ref}}{kT_{ref}} - \frac{E_g}{kT}\right] \tag{10}$$

$I_{0,ref}$, the third unknown parameter in the model, is the diode saturation current for the cell temperature at SRC, T_{ref}. E_g is the bandgap energy [eV]. Kim et al. (2009) defines the value for E_g for silicon to be

$$E_g = 1.16 - 7.02 \times 10^{-4}\left(\frac{T^2}{T - 1108}\right) \tag{11}$$

Fig. 3 shows the relationship between the bandgap energy, E_g, and temperature T.

3.4. Temperature of cell T

Variation in cell temperature occurs due to changes in the ambient temperature as well as changes in the insolation. Masters (2004) defines the cell temperature, T, as:

$$T = T_{amb} + \left(\frac{NOCT - 20\ ^\circ\mathrm{C}}{0.8}\right)G \tag{12}$$

where T_{amb} is the ambient temperature and $NOCT$ represents the nominal operating cell temperature provided by the manufacturer. G represents the solar irradiation at the ambient temperature, T_{amb}. Duffie and Beckman (2006) proposed a different formulation for the cell temperature by including heat transfer effects in the form of heat loss coefficients. The cell temperature, T, is given by:

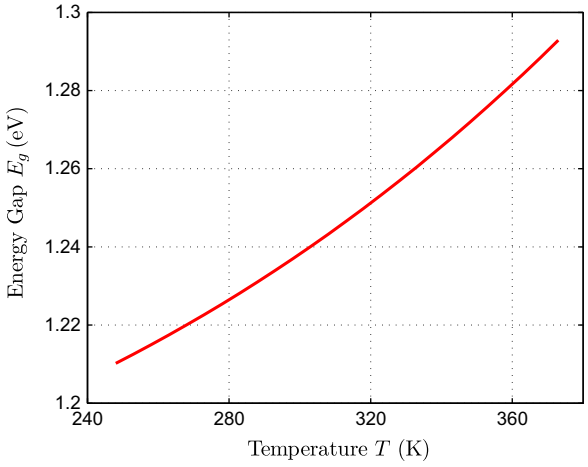

Fig. 3. Bandgap energy (E_g) versus temperature.

$$\frac{T - T_a}{T_{NOCT} - T_{a,NOCT}} = \frac{G_T}{G_{NOCT}}\frac{U_{L,NOCT}}{U_L}\left[1 - \frac{\eta_c}{(\tau\alpha)}\right] \tag{13}$$

where T_a is the ambient temperature, T_{NOCT} is the nominal operating cell temperature, $T_{a,NOCT} = 20\ ^\circ\mathrm{C}$, G_T is the solar irradiation at the ambient temperature, $G_{NOCT} = 800\ \mathrm{W/m^2}$, $U_{L,NOCT}$ and U_L are the loss coefficients at $NOCT$ and operating temperature conditions respectively, η_c is the efficiency of the cell at the temperature T, and $(\tau\alpha)$ is the absorptance–emittance product. Davis et al. (2001) proposed an equation for the cell temperature T that was derived from an analysis similar to Duffie and Beckman (2006) and is given by

$$T = \frac{G}{G_{NOCT}}(NOCT - T_{ambient,NOCT})\left(1 - \frac{\eta_c}{\tau\alpha}\right) + T_{ambient} \tag{14}$$

where G is the same as G_T, $NOCT$ is the same as T_{NOCT}, and $T_{ambient,NOCT}$ is the same as $T_{a,NOCT}$. The other variables are identical to those given in (13).

All three equations give similar results for the predicted cell temperature. Calculation of cell temperature using either (13) or (14) is problematic since $(\tau\alpha)$, η_c, $U_{L,NOCT}$ and U_L are rarely known. Thus, for this study (12) will be used.

3.5. Parallel leakage resistance R_P and series resistance R_S

The parallel leakage resistance or shunt resistance R_P and series resistance R_S are the last two unknown parameters in the cell-to-module-to-array model. As an approximation,

$$R_P > \frac{10V_{OC}}{I_{SC}} \tag{15}$$

where V_{OC} and I_{SC} are open circuit voltage and short circuit current respectively.

Desoto et al. (2006) used the following relationship relating the shunt resistance to irradiation at operating conditions and SRC,

$$\frac{R_P}{R_{P,ref}} = \frac{G}{G_{ref}} \tag{16}$$

Finally,

$$R_S < \frac{0.1 V_{OC}}{I_{SC}} \tag{17}$$

In the five parameter method outlined by Desoto et al. (2006), the series resistance is assumed to be independent of temperature and irradiation at both operating conditions and SRC,

$$R_S = R_{S,ref} \tag{18}$$

4. Datasheet based parameter determination model

In (5), there are five unknown parameters at SRC: $I_{irr,ref}$, $I_{0,ref}$, n_{ref}, $R_{P,ref}$ and $R_{S,ref}$. Solving for these five parameters using the modified current–voltage relationship requires using the mathematical model outlined by Desoto et al. (2006). This model uses data provided by the manufacturer and as mentioned before agrees well with actual measured results. The data is provided under SRC except for the variable $NOCT$, which is given for nominal operating conditions (800 W/m^2 and AM 1.5). Some manufacturers provide data for the panel under nominal operating conditions.

The model is thus a system of five equations with five unknowns. The first equation is derived from open-circuit conditions at SRC where $I_A = 0$ and $V_A = V_{OC,ref}$. Thus (5) becomes

$$0 = N_P I_{irr,ref} - N_P I_{0,ref}\left[\exp\left(\frac{qV_{OC,ref}}{N_S n_{ref} kT_{ref}}\right) - 1\right] - \frac{V_{OC,ref}}{\frac{N_S}{N_P} R_{P,ref}} \tag{19}$$

The second equation occurs at short-circuit conditions at SRC where $I_A = I_{SC,ref}$, and $V_A = 0$. Thus (5) becomes

$$I_{SC,ref} = N_P I_{irr,ref} - N_P I_{0,ref}\left[\exp\left(\frac{qI_{SC,ref} R_{S,ref}}{N_P n_{ref} kT_{ref}}\right) - 1\right] - \frac{I_{SC,ref}\frac{N_S}{N_P} R_{S,ref}}{\frac{N_S}{N_P} R_{P,ref}} \tag{20}$$

The measured current–voltage pair at the maximum power point under SRC can be substituted into (5) to obtain the third equation where $I_A = I_{mp,ref}$ and $V_A = V_{mp,ref}$,

$$I_{mp,ref} = N_P I_{irr,ref} - N_P I_{0,ref}\left[\exp\left(\frac{q(V_{mp,ref} + I_{mp,ref}\frac{N_S}{N_P} R_{S,ref})}{N_S n_{ref} kT_{ref}}\right) - 1\right] - \frac{V_{mp,ref} + I_{mp,ref}\frac{N_S}{N_P} R_{S,ref}}{\frac{N_S}{N_P} R_{P,ref}} \tag{21}$$

At the maximum power point, the derivative of power with respect to voltage is equal to zero. If at SRC, $\frac{\partial P}{\partial v}\big|_{P=P_{max},SRC} = 0 (P = V_A I_A)$ the fourth equation will be

$$\frac{I_{mp,ref}}{V_{mp,ref}} = \frac{\frac{qN_P I_{0,ref}}{N_S n_{ref} kT_{ref}} \exp\left(\frac{q(V_{mp,ref} + I_{mp,ref}\frac{N_S}{N_P} R_{S,ref})}{N_S n_{ref} kT_{ref}}\right) + \frac{1}{\frac{N_S}{N_P} R_{P,ref}}}{1 + \frac{qI_{0,ref} R_{S,ref}}{n_{ref} kT_{ref}} \exp\left(\frac{q\left(V_{mp,ref} + I_{mp,ref}\frac{N_S}{N_P} R_{S,ref}\right)}{N_S n_{ref} kT_{ref}}\right) + \frac{R_{S,ref}}{R_{P,ref}}} \tag{22}$$

The fifth and final equation ensures that the temperature coefficient of open-circuit voltage (β_T) is correctly predicted by the model,

$$\beta_T = \frac{\partial V_{OC}}{\partial T} \approx \frac{V_{OC} - V_{OC,ref}}{T - T_{ref}} \tag{23}$$

$$V_{OC} = V_{OC,ref} + \beta_T (T - T_{ref}) \tag{24}$$

β_T is the absolute temperature coefficient of the open-circuit voltage. Some manufacturers only provide the relative temperature coefficient of the open-circuit voltage, β'_T. The relationship between them is given by

$$\beta_T = \beta'_T V_{OC,ref} \tag{25}$$

In Eq. (24), the variable V_{OC} represents the open-circuit condition at the cell temperature T. A cell temperature of $T = T_{ref} \pm 10$ K should be used, since choosing 1 to 10 K above or below T_{ref} results in the same answer. Now, V_{OC} at some cell temperature T can be obtained from (5) using the same method in deriving (19). Thus,

$$0 = N_P I_{irr} - N_P I_0\left[\exp\left(\frac{qV_{OC}(T)}{N_S nkT}\right) - 1\right] - \frac{V_{OC}(T)}{\frac{N_S}{N_P} R_P} \tag{26}$$

The variables I_{irr}, I_0, R_P, n are the photocurrent, diode saturation current, and shunt resistance at the cell temperature T, respectively. When solving for the reference parameters ($I_{irr,ref}$, $I_{0,ref}$, n_{ref}, $R_{P,ref}$, $R_{S,ref}$) the solar irradiation is assumed equal ($G = G_{ref}$). We make the following substitutions in (26): (8) for I_{irr}, (10) and (11) for I_0, (16) for R_P, (7) for n, and the term $V_{OC}(T)$ from (24). After the necessary substitutions, the fifth and final condition can be written in terms of the reference parameters only.

The five Eqs. (19), (20), (21), (22) and (26) can now be solved simultaneously for the five parameters at reference conditions. These equations were solved using the nonlinear equation solver fsolve in MatLab. Once all of the parameters at reference conditions are obtained, the

cell-to-module-to-array model can predict the performance of an array of any size under different operating conditions.

Sometimes it is desirable to find the short-circuit current, and the voltage and current at the maximum power point, under cell temperature and irradiation values different from reference conditions. The short-circuit current at any operating condition is given by,

$$I_{SC} = N_P I_{irr} - N_P I_0 \left[\exp\left(\frac{qI_{SC}R_S}{N_P nkT}\right) - 1\right] - \frac{I_{SC}R_S}{R_P} \tag{27}$$

Maximum power point current and voltage at any operating condition can be obtained by simultaneously solving the following two equations using fsolve in MatLab/Simulink,

$$I_{mp} = N_P I_{irr} - N_P I_0 \left[\exp\left(\frac{q(V_{mp} + I_{mp}\frac{N_S}{N_P}R_S)}{N_S nkT}\right) - 1\right] - \frac{V_{mp} + I_{mp}\frac{N_S}{N_P}R_S}{\frac{N_S}{N_P}R_P} \tag{28}$$

$$\frac{I_{mp}}{V_{mp}} = \frac{\frac{qN_P I_0}{N_S nkT}\exp\left(\frac{q(V_{mp}+I_{mp}\frac{N_S}{N_P}R_S)}{N_S nkT}\right) + \frac{1}{\frac{N_S}{N_P}R_P}}{1 + \frac{qI_0 R_S}{nkT}\exp\left(\frac{q\left(V_{mp}+I_{mp}\frac{N_S}{N_P}R_S\right)}{N_S nkT}\right) + \frac{R_S}{R_P}} \tag{29}$$

5. Results

The cell-to-module-to-array model was tested for twenty panels, and yielded results consistent with experimental data provided by manufacturers under a wide range of cell temperatures and irradiation values. For brevity, the results for three PV modules are provided here. The modules include BP Solar's BP 3 Series 235 W PV module, ET Solar's ET Black Module ET-M572190BB and Kyocera's KD210GX-LP high efficiency multicrystal PV module.

Table 2 presents the calculated reference parameters for the BP 3 Series 235 W, ET-M572190BB and KD210GX-LP modules. Due to the nonlinear nature of the equations, the simulation results for a PV array are particularly sensitive to the values of the parameters at reference conditions. Without accurate reference parameters, it is impossible to define the characteristics of the *V–I* curve for operating conditions. The parameters in Table 2 have an explicit physical meaning intrinsic to a specific PV panel.

Fig. 4 presents the model *V–I* curves for BP Solar's BP 3 Series 235 W panel at a cell temperature of 25 °C and solar irradiation at five levels: 1000 W/m^2; 800 W/m^2; 600 W/m^2; 400 W/m^2 and 200 W/m^2. The *V–I* curves and values for the short-circuit current and open-circuit voltage compare favorably with published values.

Table 2
Calculated reference parameters for BP Solar's BP 3 Series 235 W, ET Solar's ET-M572190BB and Kyocera's KD210GX-LP modules.

Parameters	BP 3 Series 235 W	ET-M572190BB	KD210GX-LP
$I_{irr,ref}$	8.487	5.565	8.596
$I_{0,ref}$	6.330×10^{-9}	1.774×10^{-9}	6.230×10^{-9}
$R_{S,ref}$	5.125×10^{-3}	6.946×10^{-3}	5.035×10^{-3}
$R_{P,ref}$	5.837	7.287	2.711
n_{ref}	1.149	1.118	1.138

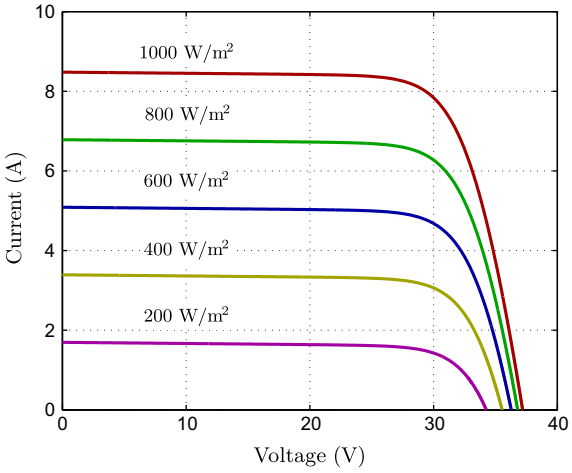

Fig. 4. Calculated *V–I* curves for BP Solar's BP 3 Series 235 W PV module at a cell temperature of 25 °C and solar irradiation at five levels: 1000 W/m^2; 800 W/m^2; 600 W/m^2; 400 W/m^2 and 200 W/m^2.

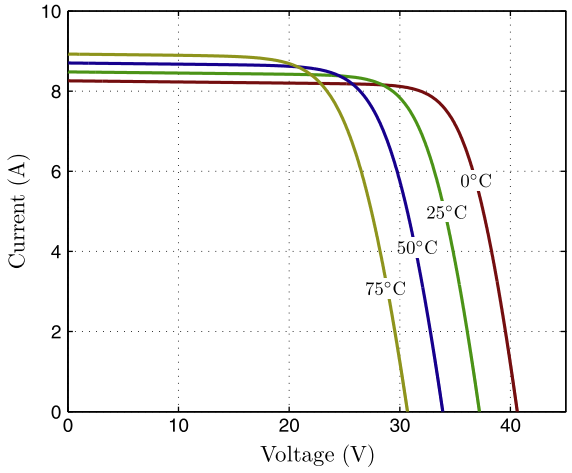

Fig. 5. Calculated *V–I* curves for BP Solar's BP 3 Series 235 W PV panel at an irradiation level of 1000 W/m^2 and cell temperatures: 0 °C; 25 °C; 50 °C and 75 °C.

Fig. 5 presents the *V–I* curves produced from the model for BP 3 Series 235 W panel at the same irradiation level of 1000 W/m^2, but with varying cell temperatures: 0 °C; 25 °C; 50 °C and 75 °C. The model results are again consistent with published values.

To check the model's ability to predict the output power and values for V_{OC} and I_{SC}, further calculations were made under both Standard Reference Conditions (SRCs) and Nominal Operating Conditions (NOCTs). Table 3 compares the model values for P_{max}, I_{mp}, V_{mp}, V_{OC} and I_{SC} with values published by the manufacturers.

For ET Solar's ET-M572190BB PV module, Fig. 6 presents *V–I* and *P–V* curves at a fixed cell temperature of 25 °C and different irradiation levels. The maximum power point for each condition is given on each curve and the

Table 3
Predicted and published results from the manufacturer under SRC and NOCT conditions for BP Solar's BP 3 Series 235 W and Kyocera's KD210GX-LP PV modules. $T_{NOCT} = 47$ °C for BP 3 Series 235 W module, $T_{NOCT} = 49$ °C for KD210GX-LP module.

Operating conditions	Parameter	BP 3 Series 235 W		KD210GX-LP	
		Datasheet	Model	Datasheet	Model
SRC 1000 W/m^2 25 °C	P_{max} (W)	235.12	235.1	210	210.1
	V_{mp} (V)	29.8	29.80	26.6	26.60
	I_{mp}(A)	7.89	7.890	7.90	7.900
	V_{OC} (V)	37.2	37.20	33.2	33.20
	I_{SC} (A)	8.48	8.480	8.58	8.580
NOCT 800 W/m^2 T_{NOCT}	P_{max} (W)	169.2	171.3	148	150.0
	V_{mp} (V)	26.5	26.84	23.5	23.72
	I_{mp} (A)	6.31	6.382	6.32	6.323
	V_{OC} (V)	33.8	33.85	29.9	29.96
	I_{SC} (A)	6.87	6.941	6.98	6.963

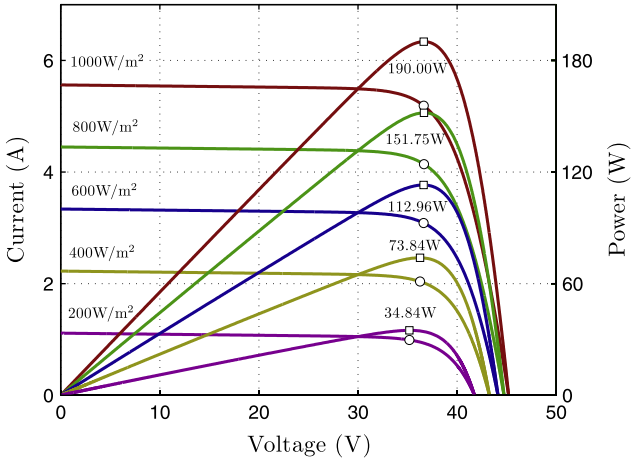

Fig. 6. Calculated V–I and P–V curves for the ET-M572190BB PV module at a cell temperature of 25 °C and solar irradiation at five levels: 1000 W/m^2; 800 W/m^2; 600 W/m^2; 400 W/m^2 and 200 W/m^2.

Table 4
Predicted maximum power point values and published results for ET-M572190BB PV panel at a cell temperature of 25 °C and solar irradiation at five levels: 1000 W/m^2; 800 W/m^2; 600 W/m^2; 400 W/m^2 and 200 W/m^2.

Irradiation (G) (W/m^2)	ET-M572190BB Datasheet	Maximum power (W) Model
1000	190.2	190.0
800	150.8	151.8
600	111.4	112.9
400	72.2	73.84
200	33.6	34.84

numerical results are published in Table 4. Comparison between these calculated maximum power point values and those published by the manufacturer reveals that they are in good agreement.

The cell-to-module-to-array model thus provides designers with a reliable and accurate method for predicting the performance of PV arrays of any size and under different operating conditions. Energy production, efficiency, maximum power, maximum power point voltage and current, short-circuit current, and open-circuit voltage are all predicted accurately for differing irradiation levels and cell temperatures. Our results reveal that through accurate calculation of reference parameters, the model can predict the V–I and P–V curves for any size array.

The modified equivalent circuit and current–voltage relationship can be easily transferred into simulation programs such as EMTDC/PSCAD and MatLab/Simulink. In EMTDC/PSCAD, the PV array model was created through a user-defined module using standard software library components. The process is straightforward and further connection with other ancillary power components that comprise the entire system is easily accomplished.

6. Experiment

Experiments were performed outdoors using four Kyocera's KC85TS PV modules installed on the roof of the North Classroom building at the University of Colorado Denver campus. A photo of the experimental setup is presented in Fig. 7. The objective was to confirm that the cell-to-module-to-array model could accurately replicate outdoor conditions for different configurations of a PV array.

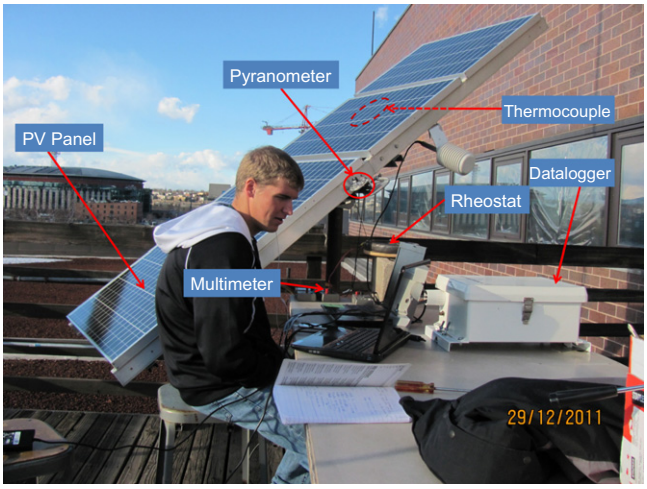

Fig. 7. Experimental device and circuit of outdoor measurement.

Solar irradiation levels were measured using the Li-COR model 200SA pyranometer and cell temperature was measured by a thermocouple attached to the rear surface of the PV module. A simple thermometer monitored the ambient temperature. Data was collected every second and averaged for the minute using a CR-10X datalogger. For the experiment, measurement of the *V–I* curve for different configurations of the four panel array was achieved through a variable resistor method. An Ohmite 45 Ω 1000 W rheostat was used to replicate the load of the array. Through variation of the resistance of the rheostat, different points on the *V–I* curve were captured using multimeters to measure the current and voltage at each point.

The experiment revealed that the specifications (P_{max}, V_{mp}, I_{mp}, I_{SC}, V_{OC}, α_T) provided by the manufacturer could not be used in the cell-to-module-to-array model to accurately replicate outdoor conditions. Possible reasons could be the method of manufacture or the age of the module. Instead, the specifications for one module of the system were calculated under an outdoor reference condition (different from SRC) and used as input for the model. Fig. 8 represents the *V–I* curve for one module under the outdoor reference condition of $G = 967.71$ W/m^2, $T = 308.82$ K.

Based on this curve, the necessary specifications were calculated (Table 5) and assumed to be representative of each of the four modules in the system.

In order to estimate the temperature coefficient of I_{SC} (α_T), the short-circuit current was measured on a clear day (January 5, 2012) from 9:35 AM to 12:32 PM. Fig. 9 reveals the tendency of the relative short-circuit current to change due to changes in solar irradiation.

The results reveal a linear relationship between short-circuit current and solar irradiation. Rearrangement of (8) led to the relationship between $\frac{I_{SC}}{I_{SC,ref}} \times \frac{G_{ref}}{G}$ and $T - T_{ref}$ as shown in Fig. 10. In this case, "*ref*" refers to the outdoor reference condition.

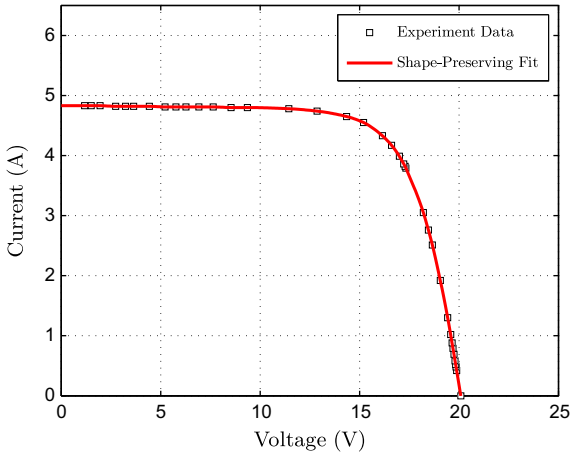

Fig. 8. *V–I* curve for one Kyocera KC85TS module under the outdoor reference condition of solar irradiation $G = 967.71$ W/m^2 and cell temperature $T = 308.82$ K.

Table 5
Calculated specifications for one Kyocera KC85TS module under the outdoor reference condition of $G = 967.71$ W/m^2, $T = 35.62$ °C (308.82 K) and ambient temperature $T_a = 14.69$ °C (287.89 K).

Specification	Calculated value
Maximum power, P_{max} (W)	69.99
Voltage at maximum power, V_{mp} (V)	15.96
Current at maximum power, I_{mp} (A)	4.38
Short-circuit current, I_{SC} (A)	4.83
Open-circuit voltage, V_{OC} (V)	20.09
Temperature coefficient of I_{SC}, α_T (A/°C)	0
Temperature coefficient of V_{OC}, β_T (V/°C)	−0.0821
Number of solar cells in series, N_S	36
Number of solar cells in parallel, N_P	2

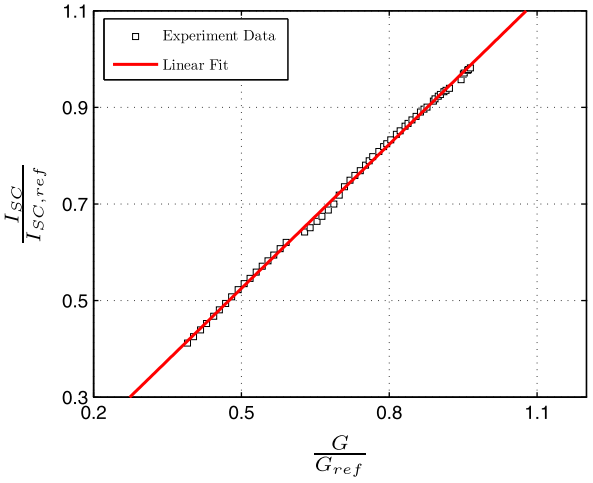

Fig. 9. Relative short-circuit current versus relative solar irradiation under outdoor condition.

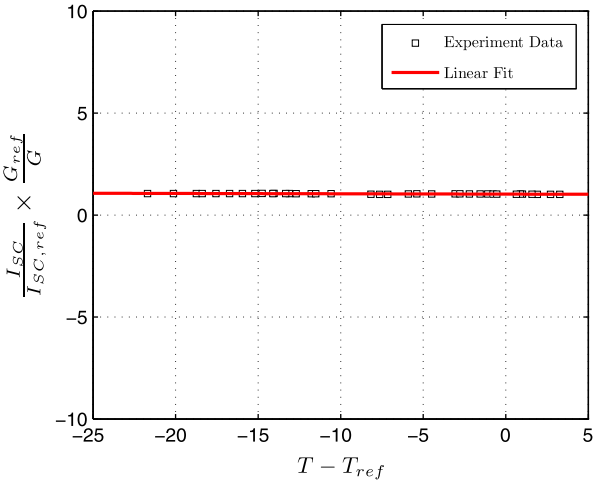

Fig. 10. Relationship between $\frac{I_{SC}}{I_{SC,ref}} \times \frac{G_{ref}}{G}$ and $T - T_{ref}$ where the slope is α'_T under the outdoor condition.

The slope of the line represents the relative temperature coefficient α'_T. From Fig. 10, it is reasonable to consider α'_T as zero and thus α_T as zero. The temperature coefficient of V_{OC} (β_T) represents the value provided by the manufacturer.

Table 6
Reference parameters for the Kyocera KC85TS module where "*ref*" refers to the outdoor reference condition.

Reference parameter	Calculated value
$I_{irr,ref}$	2.421
$I_{0,ref}$	1.996×10^{-8}
$R_{S,ref}$	1.526×10^{-2}
$R_{P,ref}$	6.462
n_{ref}	1.129

Based on the specifications given in Table 5, the reference parameters shown in Table 6 were calculated using the cell-to-module-to-array model.

After obtaining the reference parameters, comparisons between results of the outdoor experiments and the cell-to-module-to-array model were performed for three different cases: (1) PV modules wired only in parallel, including 2 modules in parallel, 3 in parallel, and 4 in parallel; (2) PV modules wired only in series, including 2 modules in series, 3 in series, and 4 in series; (3) PV modules wired in both series and parallel (2 strings of 2 modules in series in parallel).

For the first case, Figs. 11 and 12 reveal the *V–I* and *P–V* curves respectively for each instance of parallel configuration as well as the respective curves for one module.

Figs. 11 and 12 reveal consistency between experimental results (scattered points) and model results (solid line). The corresponding solar irradiation and cell temperature for each experiment are shown in Table 7 as well as the time and date of each experiment.

For the second case, Figs. 13 and 14 show the *V–I* and *P–V* curves respectively for each instance of series configuration as well as two instances for one module.

Figs. 13 and 14 reveal consistency between experimental results (scattered points) and model results (solid line). The

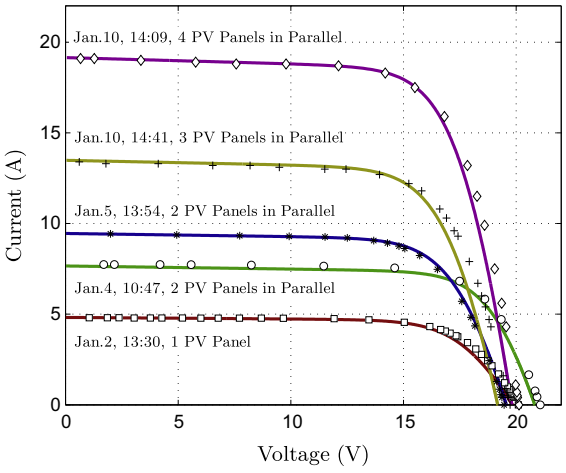

Fig. 11. Case 1: *V–I* curve comparison between experimental results (scattered points) and model results (solid line).

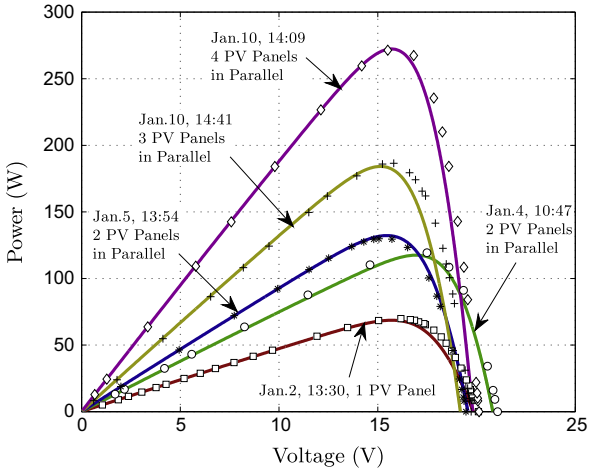

Fig. 12. Case 1: *P–V* curve comparison between experimental results (scattered points) and model results (solid line).

difference around the open-circuit voltage point in either case is due to the uncertainty of the temperature coefficient of V_{OC} (β_T). Recall that the value provided by the manufacturer was adopted for the model, which introduces some discrepancy since a "used" PV module is (to some extent) different from a "new" one. The accuracy of predicted results could be improved with a temperature coefficient of V_{OC} characteristic of the PV module. The corresponding solar irradiation and cell temperature, along with the time and date, are shown for each experiment in Table 8.

For the third case, Figs. 15 and 16 show the *V–I* and *P–V* curves respectively for PV modules wired in both series and parallel (2 strings of 2 modules in series in parallel). Once again, consistency between experimental results (scattered points) and model results (solid line) is shown.

Table 9 shows the corresponding information for each experiment.

It is clear that the model accurately predicts the *V–I* and *P–V* curves for different configurations, and thus is able to address the variation in outdoor conditions imparted by shading effects. For example, it can be beneficial to connect PV modules in parallel depending on shading effects. When the solar irradiation level is not uniform throughout the array, the contributions to the current from each PV module will be different; if connected in parallel, the different currents will not offset each other, thereby increasing overall power. In EMTDC/PSCAD a module can be defined to represent a PV array, thus adding to the convenience of simulating any sized PV array. The agreement between experimental results and model predicted results reveals the reliability and accuracy of the model.

7. Conclusion

A modified equivalent circuit and current–voltage relationship to include the effects of parallel and series connections in a PV array was derived using the single diode model for a single solar cell. This was expanded to a string

Table 7
Case 1: date, time, solar irradiation and cell temperature for each experiment.

Date	Time	Configuration	G (W/m^2)	T (K)
January 2, 2012	1:30 PM	1 Module	965.68	311.84
January 4, 2012	10:47 AM	2 Modules in parallel	767.15	296.93
January 5, 2012	1:54 PM	2 Modules in parallel	946.68	314.84
January 10, 2012	2:41 PM	3 Modules in parallel	900.59	318.84
January 10, 2012	2:09 PM	4 Modules in parallel	959.21	312.07

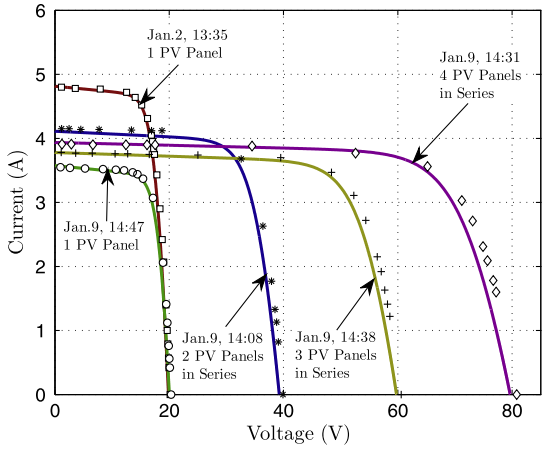

Fig. 13. Case 2: V–I curve comparison between experimental results (scattered points) and model results (solid line).

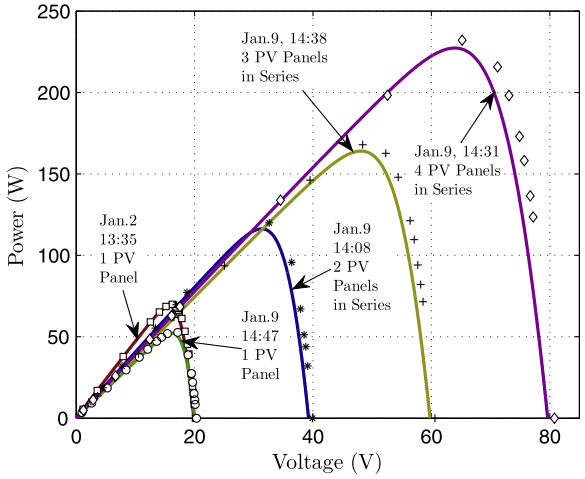

Fig. 14. Case 2: P–V curve comparison between experimental results (scattered points) and model results (solid line).

Table 8
Case 2: date, time, solar irradiation and cell temperature for each experiment.

Date	Time	Configuration	G (W/m^2)	T (K)
January 2, 2012	1:35 PM	1 Module	964.58	311.45
January 9, 2012	2:47 PM	1 Module	716.05	305.52
January 9, 2012	2:08 PM	2 Modules in series	823.67	312.19
January 9, 2012	2:38 PM	3 Modules in series	757.12	307.49
January 9, 2012	2:30 PM	4 Modules in series	788.49	308.17

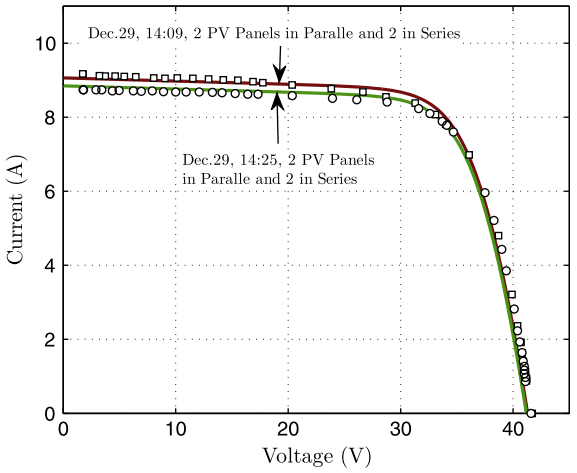

Fig. 15. Case 3: V–I curve comparison between experimental results (scattered points) and model results (solid line).

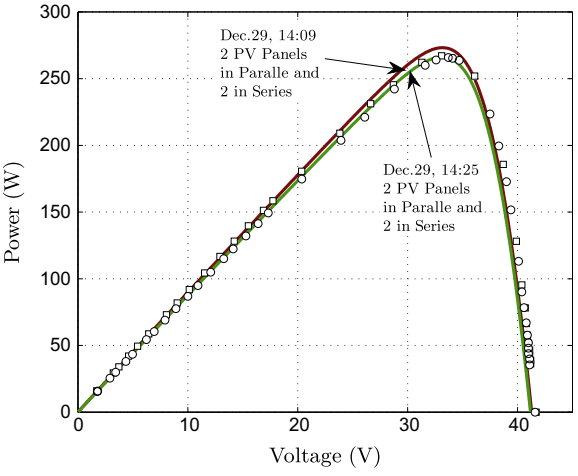

Fig. 16. Case 3: P–V curve comparison between experimental results (scattered points) and model results (solid line).

of any number of cells in series and finally to an array. Modification to the five parameter model was made because of the current–voltage relationship derived for an array, and this resulted in development of a cell-to-module-to-array model. The flexibility of this model derives from its ability to produce all important parameters and V–I and P–V curves for arrays of any size. The accuracy of the model was demonstrated by a systematic comparison of model results and published data provided by panel

Table 9
Case 3: date, time, solar irradiation and cell temperature for each experiment.

Date	Time	Configuration	G (W/m^2)	T (K)
December 29, 2011	2:09 PM	2 in Series 2 in parallel	907.72	301.30
December 29, 2011	2:25 PM	2 in Series 2 in parallel	886.22	301.58

manufacturers. The model requires information that is typically available to the designer. Model flexibility, accuracy and ease of use thus combine to give the designer a reliable prediction tool under a wide range of conditions. The modified equivalent circuit is easily used in simulation programs such as EMTDC/PSCAD and MatLab/Simulink. Validation of the accuracy of the model was shown through a series of experiments performed outdoors for different configurations of a PV array. The consistency between V–I and P–V curves for experimental and model predicted results for each configuration revealed the reliability and accuracy of the model.

Acknowledgment

We would like to thank Thomas Stoffel and Afshin Andreas at the Solar Radiation Research Laboratory from the National Renewable Energy Laboratory (NREL) for providing the equipment for our experiments.

References

Bashahu, M., Nkundabakura, P., 2007. Review and tests of methods for the determination of the solar cell junction ideality factors. Solar Energy 81, 856–863.

Cameron, C.P., Boyson, W.E., Riley, D.M., 2008. Comparison of pv system performance-model predictions with measured pv system performance. In: Photovoltaic Specialists Conference, 2008. PVSC '08. 33rd IEEE, pp. 1–6.

Campbell, R.C., 2007. A circuit-based photovoltaic array model for power system studies. 2007 39th North American Power Symposium, pp. 97–101.

Chan, D.S.H., Phang, J.C.H., 1987. Analytical methods for the extraction of solar-cell single- and double-diode model parameters from I–V characteristics. IEEE Transactions on Electron Devices 34, 286–293.

Chenni, R., Makhlouf, M., Kerbache, T., Bouzid, A., 2007. A detailed modeling method for photovoltaic cells. Energy 32, 1724–1730.

Davis, M.W., Dougherty, B.P., Fanney, A.H., 2001. Prediction of building integrated photovoltaic cell temperatures. Journal of Solar Energy Engineering 123, 200–210.

Desoto, W., Klein, S., Beckman, W., 2006. Improvement and validation of a model for photovoltaic array performance. Solar Energy 80, 78–88.

Duffie, J.A., Beckman, W.A., 2006. Solar Engineering of Thermal Processes. John Wiley & Sons, New Jersey.

Jain, A., Kapoor, A., 2004. Exact analytical solutions of the parameters of real solar cells using lambert w-function. Solar Energy Materials and Solar Cells 81, 269–277.

Jain, A., Kapoor, A., 2005. A new method to determine the diode ideality factor of real solar cell using lambert w-function. Solar Energy Materials and Solar Cells 85, 391–396.

Khezzar, R., Zereg, M., Khezzar, A. 2009. Comparative study of mathematical methods for parameters calculation of current–voltage characteristic of photovoltaic module. In: International Conference on Electrical and Electronics Engineering, 2009. ELECO 2009, pp. I-24–I-28.

Kim, S.K., Jeon, J.H., Cho, C.H., Kim, E.S., Ahn, J.B., 2009. Modeling and simulation of a grid-connected pv generation system for electromagnetic transient analysis. Solar Energy 83, 664–678.

King, D.L., 1997. Photovoltaic module and array performance characterization methods for all system operating conditions. Aip Conference Proceedings, 394, 347–368.

King, D.L., Boyson, W.E., Kratochvil, J.A., 2004. Photovoltaic array performance model. System, 39.

Masters, G.M., 2004. Renewable and Efficient Electric Power Systems. John Wiley & Sons, New Jersey.

Rajapakse, A.D., Muthumuni, D., 2009. Simulation tools for photovoltaic system grid integration studies. In: Electrical Power Energy Conference (EPEC), 2009 IEEE, pp. 1–5.

Zhou, W., Yang, H., Fang, Z., 2007. A novel model for photovoltaic array performance prediction. Applied Energy 84, 1187–1198.